

Dynamic Mechanical Analysis of Thermosetting Materials

R. Bruce Prime
IBM (Retired) / Consultant
rbprime@attglobal.net

As described in an earlier paper “Thermal Analysis in Thermoset Characterization,” thermosetting polymers are unique. Unlike thermoplastic polymers, chemical reactions are involved in their use. As a result of these reactions the materials cross-link and become “set”, i.e. they can no longer flow or dissolve.

In this paper the behavior and characteristics of thermosetting materials are briefly reviewed (see earlier paper for a more detailed discussion), followed by a detailed description of dynamic mechanical analysis of the cure process, and ending with some comments on properties of cured thermosets.

Cure is illustrated schematically in Fig. 1 for a material with co-reactive monomers such as an epoxy-diamine system. For simplicity the reaction of a difunctional monomer with a trifunctional monomer is considered. Reaction in the early stages of cure {(a) to (b)} produces larger and branched molecules and reduces the total number of molecules.

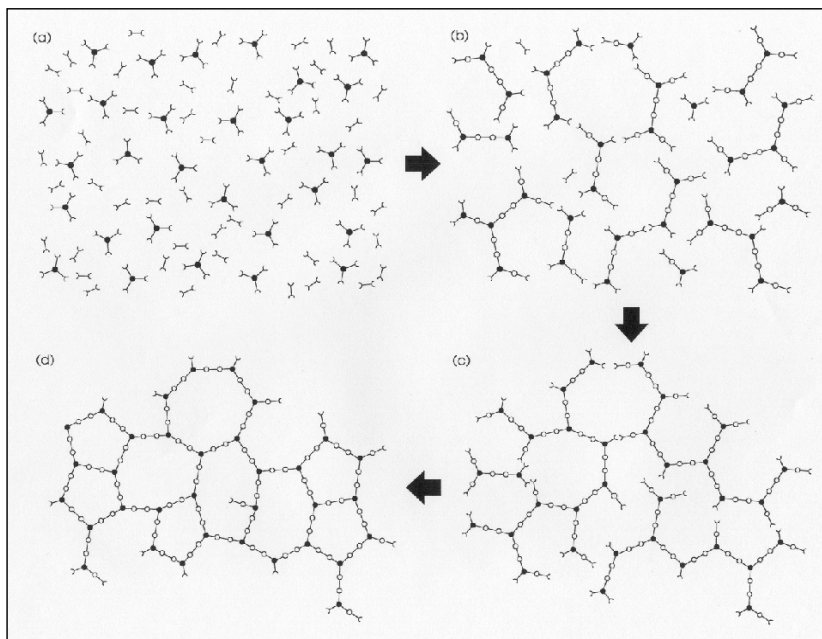


Figure 1. Schematic, two-dimensional representation of thermoset cure. For simplicity difunctional and trifunctional co-reactants are considered. Cure starts with A-stage monomers (a); proceeds via simultaneous linear growth and branching to a B-stage material below the gel point (b); continues with formation of a gelled but incompletely cross-linked network (c); and ends with the fully cured, C-stage thermoset (d). From Ref. 1.

Macroscopically the thermoset can be characterized by an increase in its viscosity η as shown in Fig. 2. As the reaction proceeds {(b) to (c)}, the increase in molecular weight accelerates and all the chains become linked together at the gel point into a network of infinite molecular weight. The gel point coincides with the first appearance of an equilibrium (or time-independent) modulus, also shown in Fig. 2. Reaction continues beyond the gel point {(c) to (d)} to complete the network formation. Macroscopically physical properties such as modulus build to levels characteristic of a fully developed network.

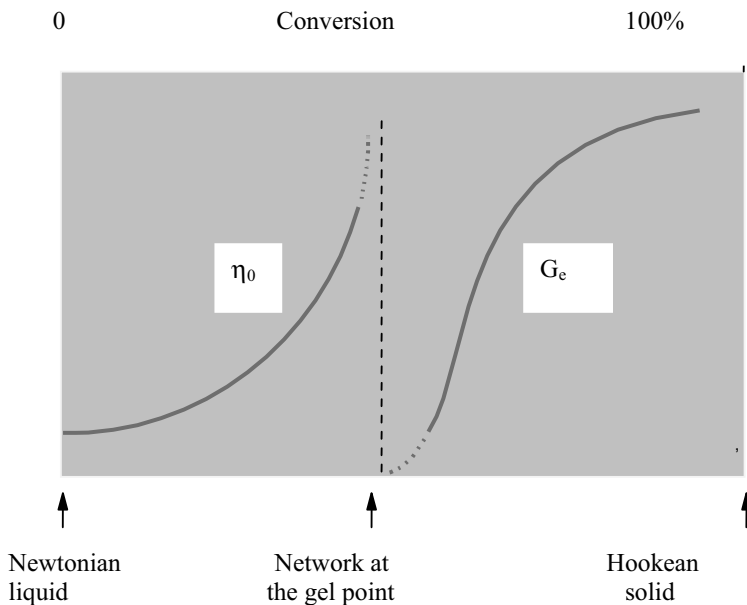
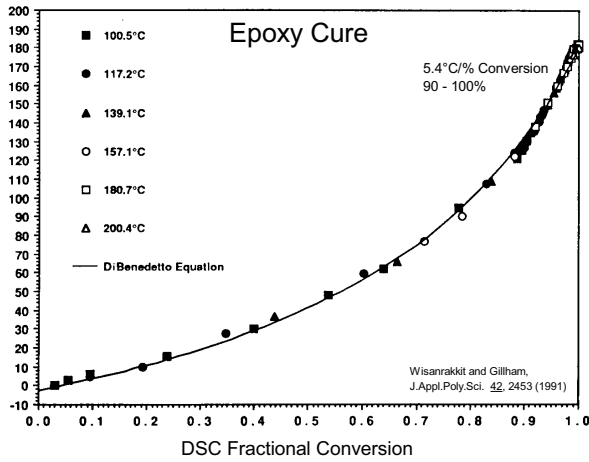


Figure 2. Macroscopic development of rheological and mechanical properties during network formation, illustrating the approach to infinite viscosity and the first appearance of an equilibrium modulus at the gel point. From Ref. 2.

Figure 2 illustrates the macroscopic progress from uncured to fully cured thermoset [2]. The uncured thermoset, often a mixture of monomers, is a Newtonian liquid. As cure progresses the viscosity increases with increasing molecular weight which can be monitored by rheological measurements. As the viscosity approaches infinity at the gel point steady shear measurements reach their limits. Oscillatory or dynamic rheology and dynamic mechanical measurements can characterize material in the gelation region. Note that while DMA may be applied to uncured materials or materials below their gel point, the samples will require a support such as metal shim, glass fabric or wire mesh. As shown in this figure, while thermosetting materials will have a dynamic modulus below the gel point, it is only above the gel point that they will have an equilibrium or time-independent modulus. DMA is especially well suited to characterize supported samples from pre-gelation, or gelled unsupported samples, to the completion of cure, as well as fully cured thermosets.



$$\ln(T_g) = \frac{(1 - \alpha) \ln(T_{g0}) + \frac{\Delta C_{p\infty}}{\Delta C_{p0}} \alpha \ln(T_{g\infty})}{(1 - \alpha) + \frac{\Delta C_{p\infty}}{\Delta C_{p0}} \alpha}$$

Venditti and Gillham, J.Appl.Poly.Sci. 64, 3, (1997)

Figure 3.

Figure 3 shows the T_g - conversion relationship for a typical epoxy-amine [3] fitted to the DiBenedetto equation [4]. Also shown is the Venditti-Gillham equation [5] relating T_g and conversion. Because of the 1:1 relationship between T_g and conversion, DMA is capable of monitoring progress of the cure reaction through measurement of T_g , as illustrated in Fig. 4. Shown are the T_g - time curves for the same epoxy system which give the same information as the conversion – time curves shown in the earlier paper.

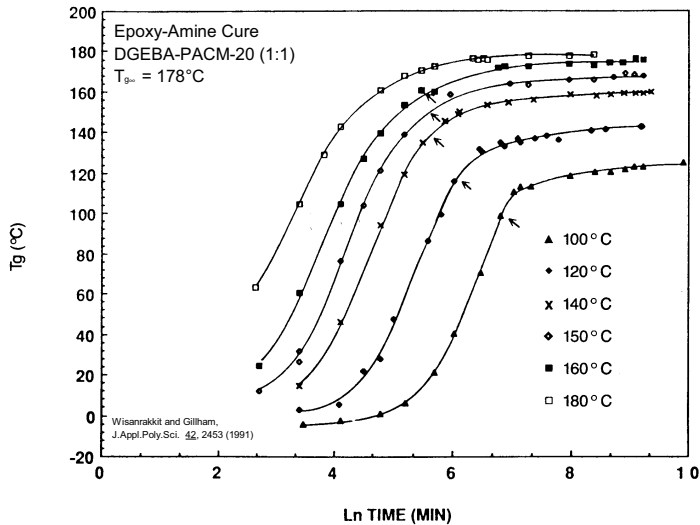


Figure 4.

To review, thermoanalytical techniques include differential scanning calorimetry (DSC), rheology, dynamic mechanical analysis (DMA), thermal mechanical analysis (TMA) and thermogravimetric analysis (TGA). DSC measures heat flow into a material (endothermic) or out of a material (exothermic). Thermoset cure is exothermic. DSC applications include measurement of T_g , conversion α , the reaction rate $d\alpha/dt$ and the heat capacity C_p . Gelation cannot be detected by DSC but vitrification can be measured by modulated-temperature DSC (MTMDSC). Rheology measures the complex viscosity in steady or oscillatory shear. In oscillatory shear the advance of cure can be monitored through the gel point and both gelation and the onset of vitrification can be detected. DMA, the subject of this paper, measures the complex modulus and compliance in several oscillatory modes. Gelation and vitrification can be detected, and the cure reaction can be monitored via T_g and beyond the gel point in the absence of vitrification via the modulus. T_g , secondary transitions below T_g , creep and stress relaxation can also be measured. TMA measures linear dimensional changes with time or temperature, sometimes under high loading. Measurements include linear coefficient of thermal expansion (CTE), T_g , creep and relaxation of stresses. TGA measures mass flow, primarily in terms of weight loss. Measurements include filler content, weight loss due to cure, outgassing, and thermal and thermo-oxidative stability.

Dynamic mechanical analysis (DMA) measures the complex modulus and compliance as a function of temperature, time and frequency. Examples of sample deformation modes include fixed frequency oscillation (single/dual cantilever, 3-point bend, tension, shear sandwich), resonant frequency oscillation, creep and stress relaxation. Thermoset properties measured include storage and loss modulus, storage and loss compliance, $\tan \delta$, T_g , secondary transitions below T_g , gelation and vitrification and reaction beyond the gel point.

In terms of modulus properties measured are

- storage modulus (E' , G') which is a measure of stress stored in the sample as mechanical energy
- loss modulus (E'' , G'') which is a measure of the stress dissipated as heat
- $\tan \delta$ ($E''/E' = G''/G'$) which is the phase lag between stress and strain, and a typical measure of damping or energy dissipation

Figure 5 illustrates typical DMA of cured thermosets. There are three regions, a glassy region which is similar for all thermosets and is characterized by very high storage modulus >1 GPa, low loss modulus and very low $\tan \delta$. A glass transition region where the storage modulus can decrease by a factor of 10 – 100 and the loss modulus and $\tan \delta$ reach maxima. And a rubbery plateau region with a stable storage modulus proportional to the cross-link density and low loss modulus and $\tan \delta$.

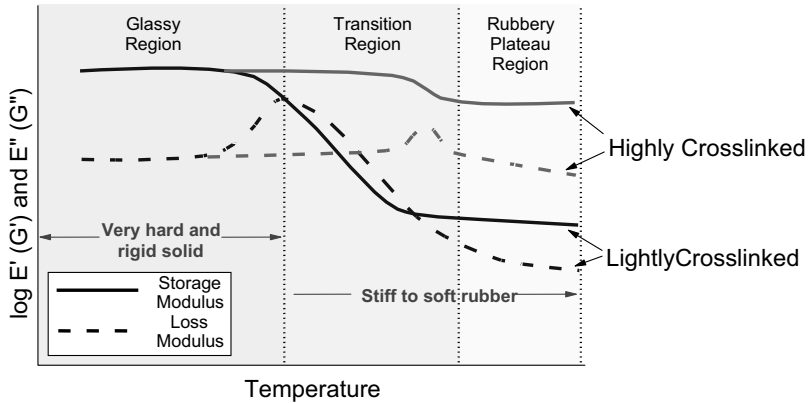


Figure 5. Schematic dynamic mechanical analysis of lightly and highly cross-linked thermosets.

For fixed frequency, DMA may be performed in single cantilever, dual cantilever, three-point bend, tensile or shear-sandwich deformation modes. Two illustrations are shown below. The first, shown in Fig. 6, is the single cantilever mode. Neat samples can be made in Teflon or silicone rubber molds, and are generally 0.5 to 2.5 mm thick. This method can be quantitative if the dimensions are precise, but it requires length correction for the clamps. For very high modulus samples the three-point bend mode may be preferred, which has the additional benefit of eliminating clamping effects.

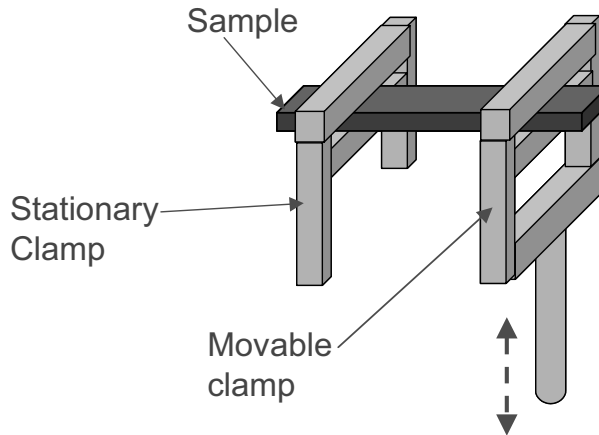


Figure 6. Single cantilever mode for dynamic mechanical analysis. Courtesy TA Instruments.

The second method illustrated is the wire mesh method, which is done on the tensile mode [1,6]. The wire mesh is usually stainless steel ~ 0.1 mm thick which may be easily coated with a liquid or paste material. The thickness is uniform and may be varied by using differing thicknesses of mesh. Because the mesh sample is mounted on a 45°

bias, where the mesh itself has almost no shear resistance, this technique gives a very sensitive measure of T_g . Semi-quantitative values G' and G'' for may be extracted via composite analysis. Samples supported on metal shim or glass fabric are normally analyzed in the dual cantilever mode.

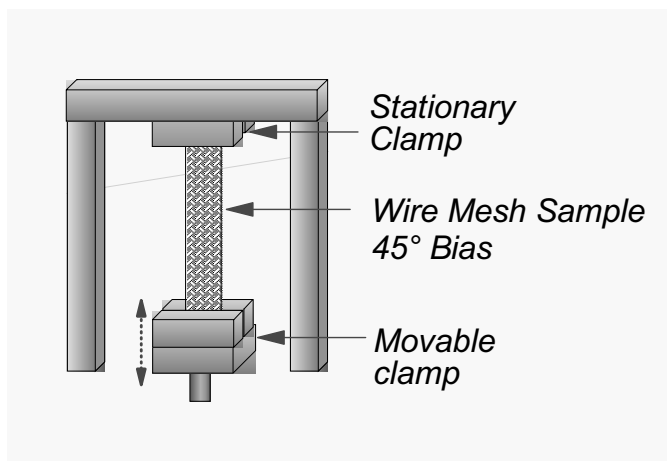


Figure 7. Wire mesh technique for dynamic mechanical analysis of liquids and pastes (1,6).

Gelation is the first appearance of a cross-linked network. It is the irreversible transformation of a liquid to a gel or rubber and it is accompanied by a small increase in the storage modulus. A distinction may be drawn between molecular or chemical gelation (the phenomenon) and macroscopic gelation (its consequence). Chemical gelation as defined by Flory is the approach to infinite molecular weight. It is an iso-conversional point (α_{gel}) that is observable as the first detection of insoluble, cross-linked gel in a reacting mixture (sol). Chemical gelation is also defined as the point where $\tan \delta$ becomes frequency independent [7]. Macroscopic gelation may be observed as the approach to infinite viscosity, the first evidence of an equilibrium modulus, the $G' = G''$ crossover in a rheology measurement, or as a loss peak in fiber and mesh supported systems.

As just mentioned the gel point is often estimated in a rheological measurement as the crossover where $G' = G''$ or $\tan \delta = 1$, as illustrated in Fig. 8 for *5 Minute Epoxy*. In this material the "5 Minutes" refers the gel point or maximum work life at room temperature, and the value measured can be seen to be very close to this time. As mentioned above a better measure is the point where $\tan \delta$ becomes frequency independent, which is usually close to but not necessarily equal to one. Note that a rubbery plateau modulus between 10^5 and 10^6 Pa is reached after long times, demonstrating that vitrification, which would result in a modulus >1 GPa, did not occur in this sample.

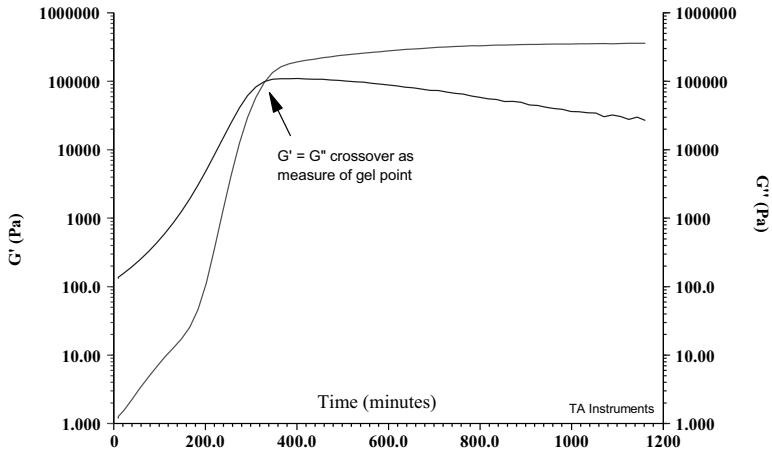


Figure 8. Dynamic rheology of 5 Minute Epoxy showing measurement of gelation.

Vitrification is glass formation due to T_g increasing from below T_{cure} to above T_{cure} as a result of reaction. It only occurs when $T_{cure} < T_{g\infty}$ and begins when $T_g = T_{cure}$ (the definition of vitrification). Vitrification is reversible by heating: liquid or gel \leftrightarrow glass. It causes a dramatic slowing of the rate of cure as a result of a shift in the reaction from chemical control to diffusion control. Vitrification is mechanically observable as a large increase in modulus and frequency dependent loss peak(s). This phenomenon is illustrated in the following two slides. It is also observable by MTDS as a step decrease in heat capacity (see earlier paper on “Thermal Analysis in Thermoset Characterization”).

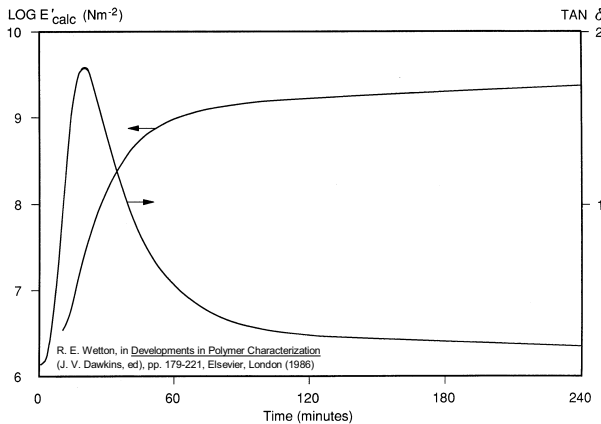


Figure 9.

Figure 9 shows the cure through vitrification at 21°C of 1 mm thick epoxy on 50 μm steel foil, coated on one side [8]. Measurements were made by DMTA at 1 Hz in the dual cantilever mode. E' and $\tan \delta$ were calculated from a composite analysis. The time

to vitrify can be taken from the peak in $\tan \delta$ at ~ 20 minutes. The rise in E' to >1 GPa confirms that the sample has vitrified.

Figure 10 shows multi-frequency DMA during isothermal cure at 40°C of an epoxy in the shear sandwich mode [9]. Vitrification is observed as a series of frequency-dependent $\tan \delta$ peaks and a frequency dependent rise in the storage modulus to ~ 1 GPa. Note that vitrification occurs at shorter times with increasing frequency, i.e. it is not isothermal. Also note the frequency independence of $\tan \delta$ initially which suggests that gelation may have occurred very early in the reaction.

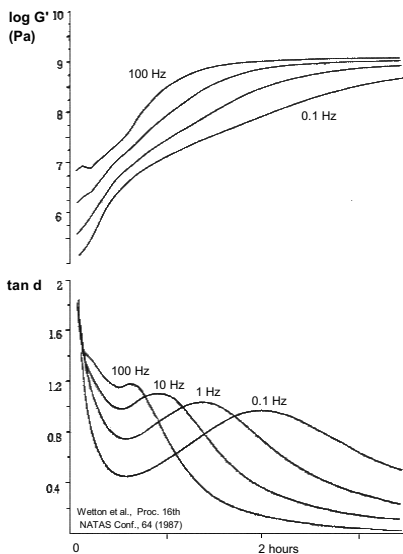


Figure 10.

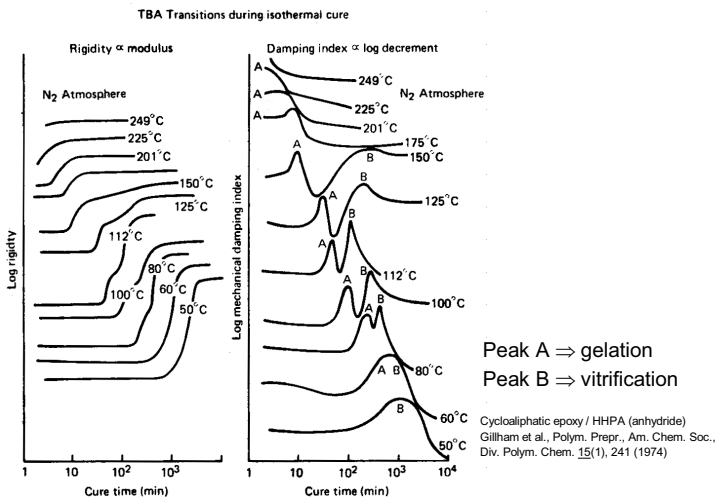


Figure 11.

Figure 11 is a classic example of gelation and vitrification during isothermal cure of an epoxy by torsional braid analysis (TBA) [10]. At 50°C the sample vitrifies and quenches the reaction prior to gelation so that only vitrification is observed. Between 80 and 150°C gelation is observed followed by vitrification. At 175°C and above only gelation is observed because the cure temperature is above $T_{g\infty}$ and the system cannot vitrify. These measurements form the basis for the construction of time-temperature-transformation (TTT) diagrams.

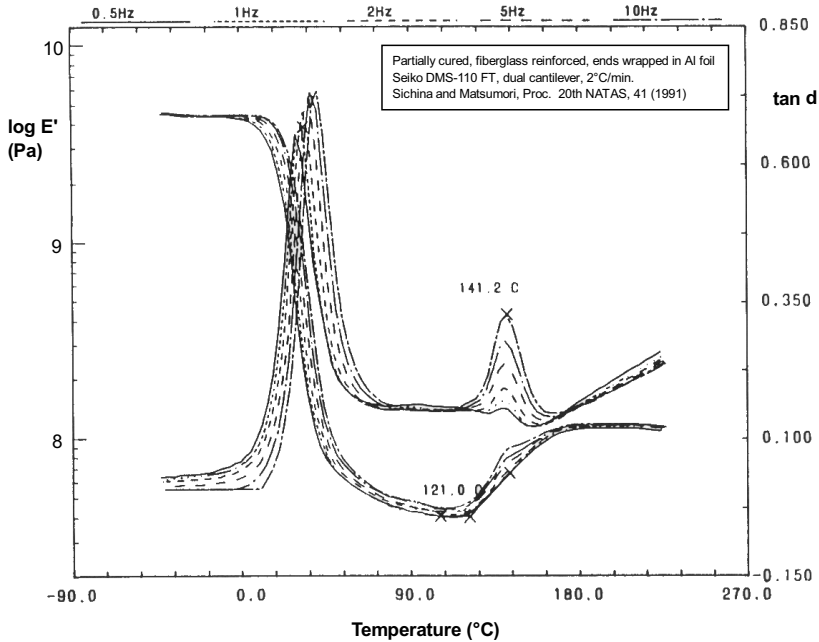


Figure 12. Multi-frequency DMA at 2°C/min of a partially cured B-staged amine-epoxy adhesive [11].

Figure 12 shows the glass transition as a series of frequency-dependent $\tan \delta$ peaks and $\sim 100\times$ decrease in storage modulus, followed by gelation near 140°C as a series of frequency-independent $\tan \delta$ peaks accompanying a small increase in modulus.

In the next section we treat kinetics by means of DMA measurements. The objective is to analyze phenomena associated with the processing and use of thermosets, which includes process life (shelf life, work life), cure, and functional life or aging. Three methodologies may be used in the study of kinetics by DMA:

- Utilize T_g as a measure of conversion
- Utilize the iso-conversional nature of gel times
- Utilize the relationship between elastic modulus and cross-link density

In Figure 13 we review from the earlier paper the use of T_g as a measure of conversion in the construction of a master cure curve at a reference temperature of 140°C showing chemical conversion as a solid line and vitrification at cure temperatures below $T_{g\infty}$ followed by diffusion controlled cure demarcated by arrows.

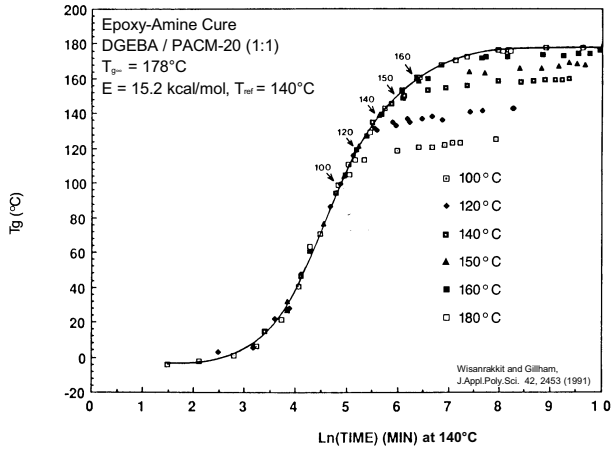


Figure 13.

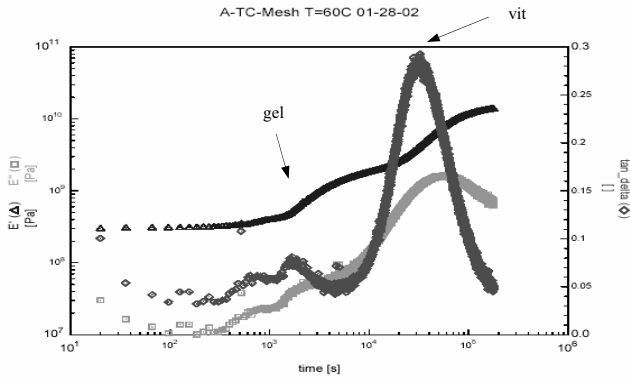


Figure 14a.

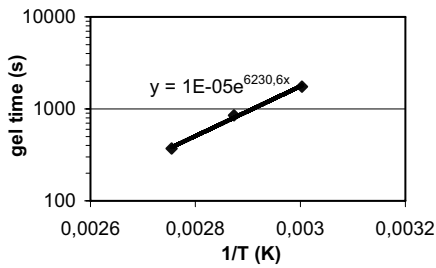


Figure 14b.

Shown in Fig. 14a is the isothermal cure at 60°C of a thermoset coating on wire mesh by DMTA [14]. Both gelation and vitrification are clearly detected. Shown in Fig. 14b is the Arrhenius plot of gel times versus cure temperature, yielding an activation energy of 12.4 kcal/mole. Figure 15 shows master cure curves of T_g versus time at 25° from time-temperature superposition of T_g – time data using the activation energy from gel times. Results are shown on two time scales, one showing several days and the other several years. While this coating would require a very long time to reach full cure at room temperature it is also to be expected that vitrification may significantly slow the reaction before complete cure ($T_g = 107^\circ\text{C}$). Note, however, that this coating reached a T_g of over 80°C at 25°C without apparent slowing of the cure process, suggesting that the diffusion controlled cure is not significantly slower than the cure under chemical control. While uncommon, this has been observed in other systems [1].

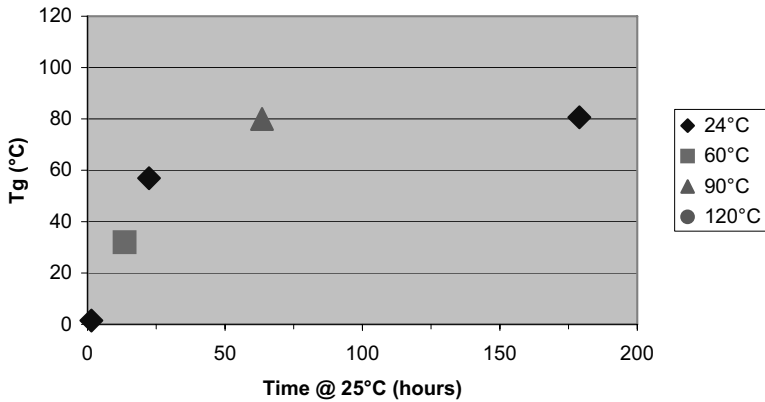


Figure 15a.

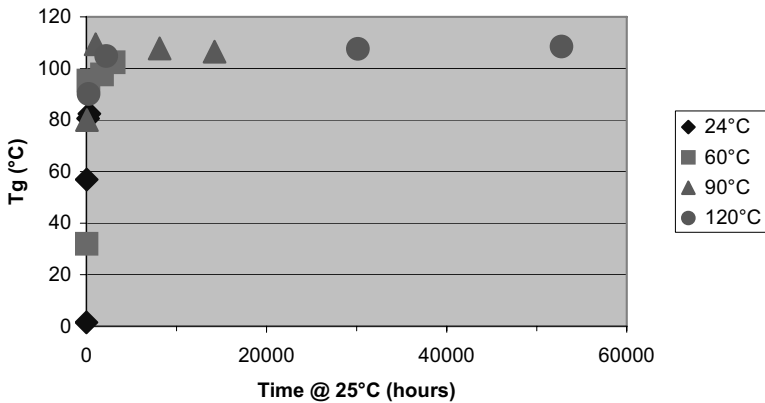


Figure 15b.

Next we utilize the relation between cross-link density and elastic modulus to measure DMA degree of cure (DOC). DOC is computed from the storage modulus (G' or E') beyond gelation in the absence vitrification [13-15] as

$$\text{DMA DOC} = (G'_i - G'_0) / (G'_{\infty} - G'_0)$$

Shown in Fig. 16 are the results of DMA DOC analyses to characterize the cure of a powder coating on wire mesh [16]. DOC – time curves were superimposed both to measure activation energy and to create the master cure curve on the right. A good correlation was observed between DOC and impact resistance and it was found that DOC was a fair predictor of other standard performance tests. DOC master curves were a much better predictor than those based on single-heating rate DSC measurements, which were found to overestimate the actual cure.

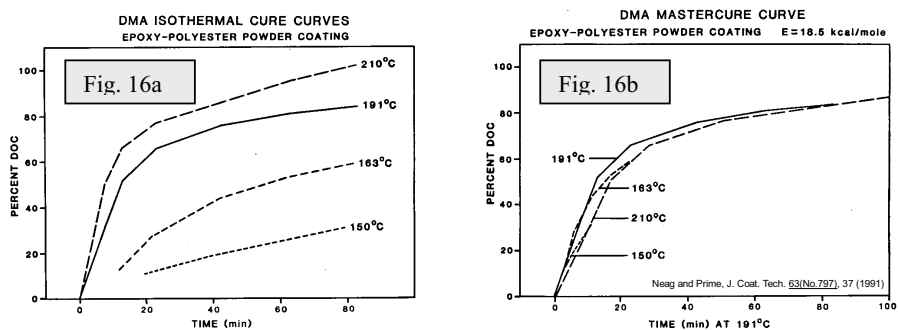


Figure 16.

The next topic is kinetic viscoelasticity, a term coined by Professor James Seferis to describe dynamic mechanical properties of reacting materials [17,18]. In kinetic viscoelasticity appropriate parameters of the viscoelastic model become functions of cure kinetics. This methodology was found to give a quantitative description of dynamic mechanical behavior during isothermal cure and a qualitative interpretation of DMA during isothermal and dynamic scans of uncured and partially cured thermosets. The next slide addresses this qualitative interpretation of DMA results, which are commonly encountered.

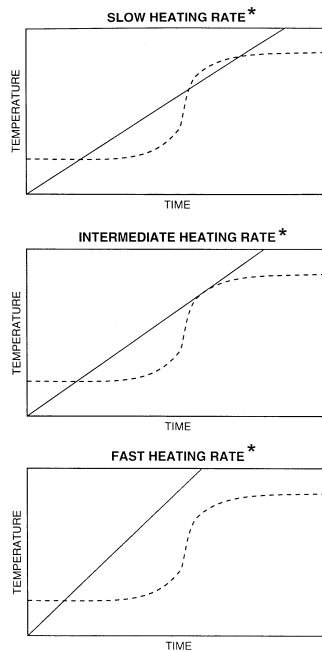


Figure 17.

In Fig. 17 the solid line is experimental temperature and the dashed line is T_g , which is increasing with cure. For the SLOW HEATING RATE (relative to reaction rate) following devitrification where the curves first cross T_g increases fast enough to cross the experimental temperature curve, whereupon the sample vitrifies. Because temperature is increasing reaction continues in the glassy state and T_g continues to rise until the reaction is complete, where the sample devitrifies on further heating. Note that there is a loss peak each time the curves cross, from either devitrification or vitrification. For the INTERMEDIATE HEATING RATE the curves just touch where vitrification and devitrification occur simultaneously. For the FAST HEATING RATE the temperature remains above T_g and reaction is completed without vitrification.

Shown in Fig. 18 is DMA of a partially cured, gelled epoxy [19]. The heating rate is $1^\circ\text{C}/\text{min}$ which is slow relative to reactivity of the thermoset. Three loss peaks were observed:

1. Devitrification of the partially cured thermoset
2. Revittrification due to reaction
3. Devitrification of the fully cured thermoset

Two loss peaks were observed in the DMA at $5^\circ\text{C}/\text{min}$, devitrification of the partially cured thermoset and revitrification near end of reaction followed immediately by devitrification at end of reaction. Only devitrification of the partially cured thermoset was observed at

10°C/min.

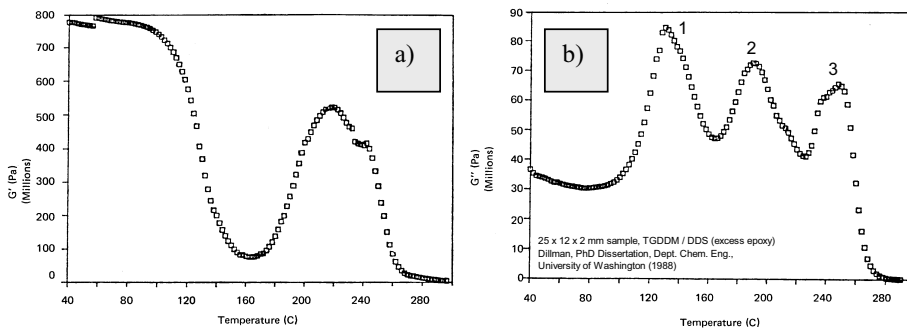


Figure 18. DMA of partially cured, gelled epoxy at 1°C/min. [19]. a) Storage modulus, b) Loss modulus

Figure 19 shows DMA of an uncured and partially cured epoxidized novolak-anhydride on wire mesh [20]. All samples were heated at 5°C/min. The uncured sample shows a small step increase in G' and a peak in G'' , indicating gelation. Focusing on the G'' curves, samples cured at 40 and 60° show two peaks, devitrification of the partially cured thermoset and a doublet where revitrification is followed almost immediately by devitrification. The 80° sample shows a merging of all peaks as heating and reaction rates are comparable. Only one very broad peak is observed in the 100° sample and the others show only devitrification. Notice the uniform increase in T_g with cure.

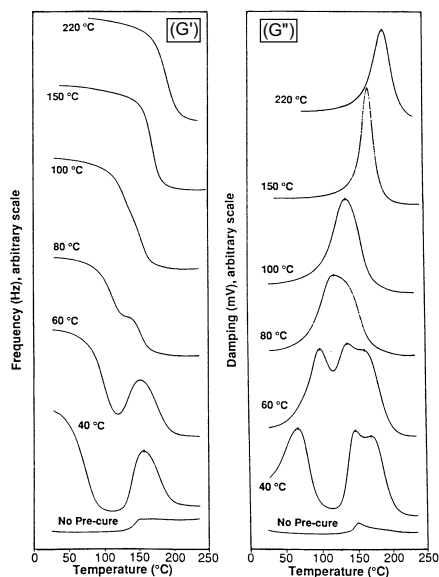


Figure 19.

The last topic covered is the DMA of cured thermosets. Properties that can be measured include:

- The glass transition T_g
- Modulus - temperature - frequency
- Physical aging¹ Time - temperature superposition
- Creep and stress relaxation²

The next slide shows the temperature – frequency behavior of a modified toughened epoxy. The temperature was raised in a step-isothermal mode with 2.5°C intervals. During the isothermal portions frequency was scanned from 0.01 to 1 Hz. The T_g for this system was 170°C, taken as the maximum in the loss modulus at 1 Hz.

The most common application of DMA to thermosets is measurement of the glass transition temperature. T_g is the transition of a glassy solid to a liquid or rubber in an amorphous material. It is accompanied by a 10 – 1000x decrease in storage modulus or increase in storage compliance. T_g is measured as the maximum in loss modulus, loss compliance or $\tan \delta$. It is a frequency dependent transition where ΔT_g is typically 5 – 6°C per decade of frequency. The glass transition is accompanied by increases in the coefficient of thermal expansion (~3x), diffusion coefficient, water sorption and transport. It is a mechanism for the relaxation of residual or stored stress where heating to just above T_g will allow those stresses to relax.

Figure 20 shows frequency multiplexing during a 1°C/min DMA scan of a moderately cross-linked epoxy [23]. Frequency was stepped between five values ranging from 0.33 to 30 Hz as the sample was heated. Both storage modulus and $\tan \delta$ can be seen to shift to higher values with increasing frequency. The typical dependence of T_g on frequency can be seen in the $\tan \delta$ data. An Arrhenius plot of $\log(\text{frequency})$ versus reciprocal absolute temperature yielded an activation energy of 383 kJ/mol for the T_g relaxation process.

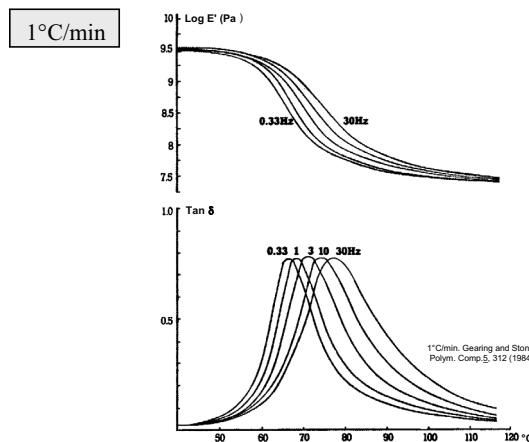


Figure 20.

¹ Consists of a densification process inherent in the nonequilibrium character of the glassy state. Takes place below T_g and is observed by DMA as an increase in modulus and decrease in damping (22).

² Creep compliance = strain(t) / stress, stress relaxation modulus = stress(t) / strain.

Time-temperature superposition is a concept that was introduced in the 1950's by Williams, Landel and Ferry [24]. It addresses the temperature dependence of relaxation processes in amorphous polymers above T_g which involves the temperature dependence of free volume. Master curves of, e.g., modulus-frequency, creep compliance and stress relaxation modulus, may be constructed over several decades of time or frequency. Master curves allow the concise presentation of all data on one curve (the "big picture") and permit behavior to be predicted at relevant conditions, e.g. over the lifetime of a structural part. The WLF equation is shown at the bottom of Fig. 21. a_T is the shift factor.

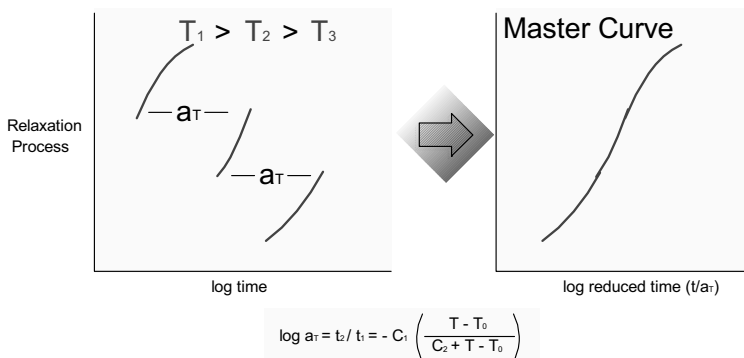


Figure 21.

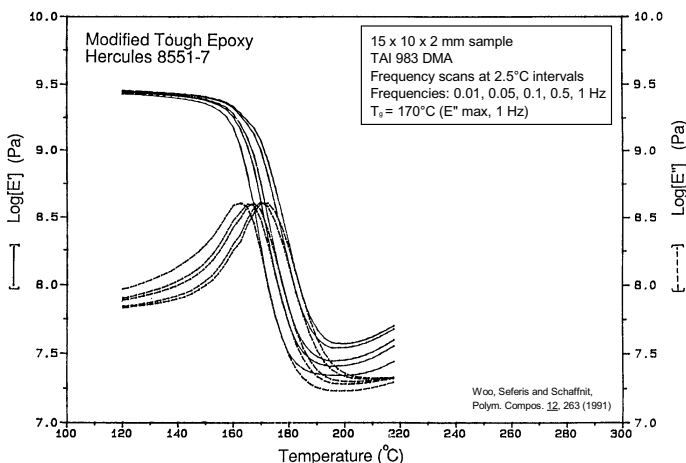


Figure 22.

Figure 22 shows the temperature – frequency behavior of a modified toughened epoxy [25]. The temperature was raised in a step-isothermal mode with 2.5°C intervals. During the isothermal portions frequency was scanned from 0.01 to 1 Hz. The T_g for this system was 170°C, taken as the maximum in the loss modulus at 1 Hz.

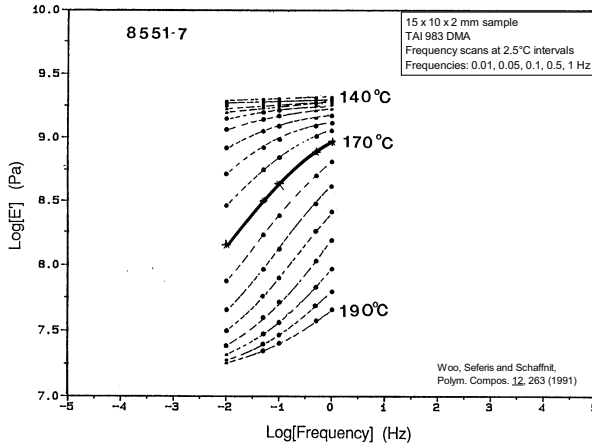


Figure 23.

Figure 23 shows the storage modulus – frequency curves through the glass transition interval [25]. Note that this is the same data shown above but plotted in a different fashion. To construct the master curves the reference curves were chosen as the storage modulus curve at 170°C (highlighted above) and the loss modulus curve at 170°C (not shown). Data >170° were shifted to the left and data <170° were shifted to the right to form the master curves of storage and loss modulus versus frequency at a reference temperature of 170°C in Fig. 24. Note that decreasing frequency is equivalent to increasing temperature. When coupled with a quantitative description of the shift factors (a_T) versus temperature, e.g. by means of the WLF equation, such master curves completely define the viscoelastic properties of a material.

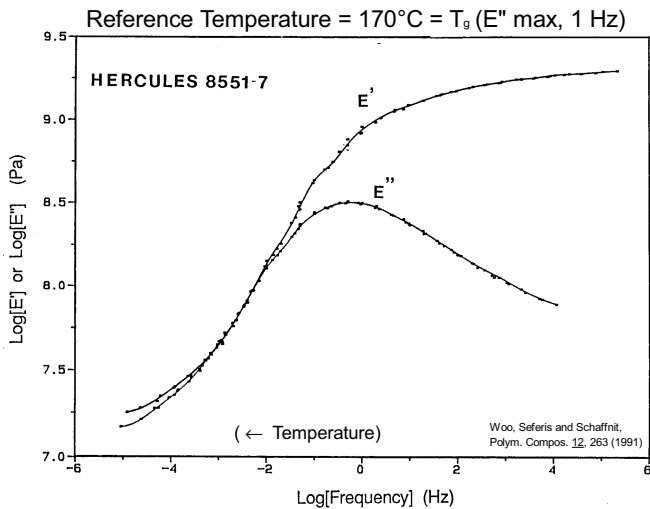


Figure 24.

Bibliography

1. R. B. Prime, Chapter 6 “Thermosets” in Thermal Characterization of Polymeric Materials (E. A. Turi, ed.) Academic Press, San Diego (1997).
2. H. H. Winter, et al. in Techniques in Rheological Measurement (A. A. Collyer, ed.) Chapman and Hall, London (1997).
3. G. Wisanrakkit and J. K. Gillham, *J. Appl. Poly. Sci.* **42**, 2453 (1991).
4. A. T. DiBenedetto, *J. Polym. Sci., Par B: Polym. Phys.* **25**, 1949 (1987).
5. R. A. Venditti and J. K. Gillham, *J. Appl. Polym. Sci.* **64**, 3 (1997).
6. S. H. Dillman, J. C. Seferis and R. B. Prime, *Proc. North Am. Therm. Anal. Soc. Conf.* **16th**, 429 (1987).
7. H. H. Winter, *Polym. Eng. Sci.* **27**, 1698 (1987).
8. R. E. Wetton, in Developments in Polymer Characterization – 5, (J. V. Dawkins, ed.), pp. 179-221. Elsevier, London (1986).
9. R. E. Wetton, P. W. Ruff, J. C. Richmond, and J. T. O’Neill, *Proc. North Am. Therm. Anal. Soc. Conf.* **16th**, 64 (1987).
10. J. K. Gillham, J. A. Benci, and A. Noshay, *Polym. Prepr., Am. Chem. Soc., Div. Polym. Chem.* **15**(1), 241 (1974).
11. W. J. Sichina and B. Matsumori, *Proc. North Am. Therm. Anal. Soc. Conf.* **20th**, 41 (1991).
12. A. T. Eng, L. M. McGrath, F. D. Pilgrim, and R. B. Prime, *North Am. Therm. Anal. Soc. Conf.* **30th**, Poster Paper (2002).
13. P. G. Babayevsky and J. K. Gillham, *J. Appl. Polym. Sci.* **17**, 2067 (1973).
14. T. Provder, R. M. Holsworth and T. H. Grentzer, *ACS Symp. Ser.* **203**, 77 (1983).
15. M. E. Koehler, A. F. Kah, C. M. Neag, T. F. Niemann, F. B. Mahili and T. Provder, *Anal. Calorim.* **6**, 361 (1984).
16. C. M. Neag and R. B. Prime, *J. Coat. Technol.* **63** (797), 37 (1991).
17. S. H. Dillman and J. C. Seferis, *J. Macromol. Sci. Chem.* **A26**, 227 (1989).
18. J.-D. Nam and J. C. Seferis, *J. Polym. Sci: Polym. Phys. Ed.*, **37**(9), 907 (1999).
19. J. C. Seferis, personal communication.
20. S. H. Dillman, Ph.D. Dissertation, Dept. Chem. Eng., University of Washington (1988).
21. N. M. Patel, C. H. Moy, J. E. McGrath, and R. B. Prime, *Proc. North Am. Therm. Anal. Soc. Conf.* **18th**, 232 (1989).
22. L. C. E. Struik, Physical Aging in Amorphous Polymers and Other Materials, Elsevier, New York (1978).
23. J. W. E. Gearing and M. R. Stone, *Polym. Compos.* **5**, 312 (1984).
24. M. L. Williams, R. F. Landel and J. D. Ferry, *JACS* **77**, 3701 (1955).
25. E. M. Woo, J. C. Seferis and R. S. Schaffnit, *Polym. Compos.* **12**, 273 (1991).